Volume 23, No 4 | International Journal of Radiation Research, October 2025

Salivary metabolomic profiling reveals dynamic metabolic adaptations in nasopharyngeal carcinoma (NPC) patients during radiotherapy

L. Ji[1], L. Wang[1], S. Qin[1], Y. Fan[2*], J. Zhou[1*]

[1]*Department of Radiation Oncology, the First Affiliated Hospital of Soochow University, Soochow, China*
[2]*Department of Hematology, the First Affiliated Hospital of Soochow University, Soochow, China*

► ***Original article***

Corresponding authors:
Yi Fan, M.D. & Juying Zhou, M.D.,
E-mail: *yifan.suda@vip.163.com*
zhoujuyingsy@163.com

Received: April 2024
Final revised: May 2025
Accepted: May 2025

Int. J. Radiat. Res., October 2025; 23(4): 855-864

DOI: 10.61186/ijrr.23.4.4

Keywords: *Nasopharyngeal neoplasms, radiotherapy, metabolomics, saliva, metabolic networks and pathways.*

ABSTRACT

Background: Nasopharyngeal carcinoma (NPC) is commonly treated with radiotherapy, which can induce systemic and local metabolic changes. Saliva, as a non-invasive biofluid, provides a valuable medium for monitoring such alterations. This study aimed to investigate salivary metabolic changes in NPC patients before and after radiotherapy using an untargeted metabolomics approach. ***Materials and Methods:*** Saliva samples were collected from 23 NPC patients both prior to and following radiotherapy. An untargeted metabolomics analysis was performed using liquid chromatography-tandem mass spectrometry (LC-MS/MS). Multivariate statistical analysis was employed to identify differential metabolites, and pathway enrichment analysis was conducted to elucidate the affected biological processes. Key metabolic features were selected using least absolute shrinkage and selection operator (LASSO) regression. ***Results:*** A total of 110 differential metabolites were identified, comprising 64 in positive ion mode (30 upregulated, 34 downregulated) and 46 in negative ion mode (31 upregulated, 15 downregulated). LASSO analysis highlighted four key metabolites: L-Carnitine and Kanosamine were significantly upregulated post-radiotherapy, whereas Phloroglucinol and Dibutyl phthalate were significantly downregulated. Pathway enrichment analysis revealed five significantly affected pathways: arginine biosynthesis, central carbon metabolism in cancer, arginine and proline metabolism, HIF-1 signaling pathway, and protein digestion and absorption. ***Conclusion:*** Salivary metabolomics revealed notable metabolic adaptations in NPC patients following radiotherapy, reflecting tissue repair and compensatory responses. These findings provide new insights into the metabolic impact of radiotherapy and may help identify potential therapeutic targets for optimizing treatment outcomes.

INTRODUCTION

Nasopharyngeal carcinoma (NPC) is a malignant tumor arising from the epithelial lining of the nasopharynx, with a notably high prevalence in East and Southeast Asia [1, 2]. Due to its anatomical location and high radiosensitivity, radiotherapy (RT) remains the standard and most effective primary treatment modality for NPC [3-5]. Despite its therapeutic benefits, RT often leads to adverse effects, particularly radiation-induced oral mucositis (RIOM)-a debilitating inflammatory condition of the oral mucosa that significantly impacts patient comfort, nutrition, and treatment adherence [6-8].

The pathophysiology of RIOM is complex and involves a cascade of biological events including the activation of inflammatory pathways, generation of reactive oxygen species, DNA damage, and tissue remodeling. These events are tightly linked with dynamic changes in cellular metabolism, which manifest through altered metabolic products and biochemical pathways. However, most conventional studies have focused on isolated inflammatory or molecular markers, lacking a systems-level view of the metabolic landscape associated with RT [6-8].

Saliva has emerged as a promising, non-invasive biofluid for monitoring local and systemic physiological changes. Produced by salivary glands, it contains a wide range of biomolecules, including enzymes, cytokines, hormones, and metabolites, reflecting both oral and general health status [9]. Its easy accessibility makes it particularly suitable for longitudinal monitoring of treatment-related changes, especially in head and neck cancer patients [10].

Metabolomics, the comprehensive analysis of low-molecular-weight metabolites in biological samples, offers unique insights into cellular responses and disease mechanisms. In particular, untargeted metabolomics, which employs advanced platforms such as liquid chromatography–tandem mass spectrometry (LC-MS/MS), allows for unbiased detection of metabolic shifts without prior knowledge of the compounds involved. When applied to saliva, this technique enables the detection of metabolic perturbations caused by disease progression,

[DOI: 10.61186/ijrr.23.4.4]

microbial imbalances, or therapeutic interventions [11-13].

Recent studies have explored the salivary metabolome in various oral and systemic diseases; however, investigations focusing on the salivary metabolic impact of RT in NPC patients are scarce. Some preliminary research suggests that RT can alter key metabolites involved in inflammation, oxidative stress, and tissue regeneration, but comprehensive profiling and pathway-level analysis remain limited [9, 10]. Given the dynamic metabolic changes that occur during RT, a deeper understanding of these alterations could facilitate the identification of predictive biomarkers and inform supportive care strategies.

In this study, we applied untargeted salivary metabolomics using LC-MS/MS to investigate the metabolic changes in NPC patients undergoing RT. By analyzing pre- and post-treatment saliva samples from the same individuals, we aimed to identify significantly altered metabolites and elucidate the affected metabolic pathways.

The aim of this study was to characterize salivary metabolic alterations associated with radiotherapy in nasopharyngeal carcinoma patients and to identify key metabolites and biological pathways involved in tissue response and repair. This work provides novel insights into the systemic effects of radiotherapy and highlights potential biomarkers for improving the prediction and management of RT-related complications.

MATERIALS AND METHODS

Study subjects

This study retrospectively collected saliva samples from 23 patients diagnosed with nasopharyngeal carcinoma (NPC) who underwent radical radiotherapy at the Department of Radiation Oncology, First Affiliated Hospital of Soochow University, between January and June 2023. Saliva samples were obtained on the first day (AF group) and the last day (ES group) of radiotherapy for each patient. Within this study group, 16 patients were male, with a mean age of 58.81 ± 8.17 years, whereas 7 patients were female, averaging 52.86 ± 11.15 years. The Medical Ethics Committee of the aforementioned hospital rigorously reviewed and approved this study (Approval number: (2024) Lunyan Approval No. 048).

Inclusion criteria

Inclusion criteria included: The patient was diagnosed with nasopharyngeal carcinoma based on pathological findings. Ages spanned from 20 to 70 years; Body mass index (BMI): 16.5 to 25.6 kg/m^2; Dietary regimen: a traditional Chinese diet was adhered to for all three meals. Previous medication history included no use of antibiotics, antimalarials, antacids, or receptor antagonists within one week prior to sampling; participants refrained from using steroid medications or non-steroidal anti-inflammatory drugs (NSAIDs), such as aspirin, in the month prior to sample collection. Medical history revealed no other systemic diseases and no additional oral mucosal conditions. No moderate or severe periodontal disease was identified.

Saliva sample collection

In accordance with Rhodus' modified method [12 9], unstimulated whole samples of saliva were collected from participants between 9:00 am and 11:00 am, following a one-hour fasting period. Participants were instructed to hold the saliva in their mouths for at least 1 minute before expectorating whole saliva into a sterile centrifuge tube, ensuring no mucus was included. Standardized protocols ensured the acquisition of adequate biospecimen volumes (2-5 mL) through iterative collection procedures as required. Immediately after collection, oral fluid specimens were stabilized on ice and transported to the analytical facilities for cryopreservation. Initial processing involved cold-chain centrifugation at 4°C, 5000 ×g for 10 minutes to separate cellular components from soluble fractions. The acellular supernatant was then sterile-filtered using 0.22 μm pore size filters (Millipore, USA) to remove particulate contaminants prior to aliquot preparation. For long-term storage, 1 mL aliquots of the clarified filtrate were aseptically transferred into pre-labeled cryovials (Thermo Fisher Scientific, USA) and stored at ultralow temperatures (-80°C) to maintain biochemical stability. Prior to untargeted metabolomics analysis, saliva samples were thawed. To minimize variability, all sample collections were performed by a single operator. LC-MS/MS analysis, data processing, and interpretation were conducted at Suzhou Meixin Biotechnology Co., Ltd. (Suzhou, China).

Steps in extraction and preparation of saliva metabolites

1. The experimental samples were thawed at 4°C. After thawing, they were vortexed for 1 minute to ensure thorough mixing. An accurate volume of each sample was then transferred into a 2 mL centrifuge tube. Following this, 400 μL of methanol chilled at -20°C (Merck, Germany) was added, and the contents were vortexed for another minute. The samples were subjected to centrifugation at 12,000 rpm for 10 minutes at 4°C. Following this procedure, the supernatant was carefully collected and transferred to a new 2 mL centrifuge tube for further concentration and drying.
2. Subsequently, exactly 150 μL of a pre-prepared 2-chloro-L-phenylalanine solution (4 ppm) in 80% methanol (Merck, Germany) was added to

[DOI: 10.61186/ijrr.23.4.4]

reconstitute the dried sample. The filtrate obtained from passing the solution through a 0.22 μm membrane filter (Millipore, USA) was collected in a detection vial.

A total of 50 μL from each sample was aliquoted into three plates for positive and negative ion detection; one plate served as a backup. Additionally, a 20 μL aliquot of the remaining sample was mixed for quality control (QC).

Untargeted metabolomics analysis of saliva samples

A comprehensive untargeted metabolomics analysis of saliva samples from nasopharyngeal carcinoma (NPC) patients was conducted using liquid chromatography-tandem mass spectrometry (LC-MS/MS). Data collection was carried out in both positive and negative ionization modes on a high-resolution Q Exactive 120 LC-MS/MS instrument (Thermo Fisher Scientific, USA), which expanded the range of detectable metabolites. The acquired LC-MS/MS data were subsequently processed with Compound Discoverer 3.1 software (Thermo Fisher Scientific, USA) for peak detection, retention time alignment, and metabolite annotation.

Chromatographic conditions

Sample analysis was conducted using a Waters 2D UPLC system (Waters Corporation, USA) coupled with a Q-Exactive mass spectrometer (Thermo Fisher Scientific, USA) equipped with a heated electrospray ionization (HESI) source. The instrument was operated via Xcalibur 2.3 software (Thermo Fisher Scientific, Waltham, MA, USA). Chromatographic separation was achieved on an ACQUITY UPLC® HSS T3 column (2.1 × 150 mm, 1.8 μm particle size, Waters Corporation, USA), maintained at 40°C. For positive ion mode, the mobile phase consisted of 0.1% formic acid in acetonitrile (B2) and 0.1% formic acid in water (A2), with the following gradient elution program: 0-1 min, 2%B2; 11 min, 2%B3; 1-9 min, 2%-50% B3; 9~12 min, 50%-98% B3; 12-13.5 min, 98% B3; 13.5-14 min, 98%-2% B3; 14 to 17 min, 2%B3. The flow rate was set to 0.35 mL/min, and the injection volume was 5 μL.

Mass spectrometry conditions

For both positive and negative ionization modes, the mass spectrometer was configured with the following parameters: a spray voltage of 3.50 kV for positive ions and -2.50 kV for negative ions, sheath gas flow set to 30 arbitrary units, and auxiliary gas flow set to 10 arbitrary units. The capillary temperature was maintained at 325°C. In the initial stage, full scan analysis was conducted at a resolution of 60,000 over an m/z range from 100 to 1000. For the subsequent stage, higher-energy collisional dissociation (HCD) was utilized for fragmentation, with a collision energy of 30% and a resolution of 15,000. The four most intense ions were chosen for further fragmentation, and dynamic exclusion was applied to filter out redundant MS/MS data.

To enhance experimental reliability during instrument testing, samples were analyzed in random order to minimize systematic errors; one quality control (QC) sample was included after every ten samples, followed by blank samples interspersed after each QC sample to prevent cross-contamination.

Radiotherapy treatment protocol

Radiotherapy was administered to all patients diagnosed with nasopharyngeal carcinoma (NPC) according to a standard treatment protocol at the Department of Radiation Oncology, First Affiliated Hospital of Soochow University. The treatment regimen followed a radical radiotherapy approach, utilizing external beam radiotherapy (EBRT).

1. Total Dose: The total dose of radiation delivered to each patient was 70 Gy, which is the standard dose for radical treatment in NPC. This total dose is delivered over the course of treatment to ensure effective tumor control while minimizing damage to surrounding healthy tissues.
2. Dose per Fraction: The dose was delivered in daily fractions of 2 Gy per fraction, five times a week. This fractionation schedule, a typical regimen for head and neck cancers, was chosen to maximize tumor control and minimize acute side effects.
3. Treatment Technique: Radiotherapy was performed using a Varian Clinac iX linear accelerator (Varian Medical Systems, USA), with 6 treatment fields. The treatment was planned using the Eclipse treatment planning system (Varian Medical Systems, USA), ensuring optimal tumor coverage and sparing of critical structures, such as the spinal cord and parotid glands.
4. Treatment Plan and Verification: Treatment plans were created based on diagnostic imaging, including CT scans, to delineate the tumor and surrounding organs at risk. The plans were reviewed by a multidisciplinary team including radiation oncologists, medical physicists, and dosimetrists. To verify proper delivery of radiation, portal imaging was used during the course of treatment to ensure the accuracy of radiation delivery.
5. Boosting: In cases where the tumor was located in a critical area or exhibited resistance to treatment, a boost to the tumor bed was administered. The boost dose was 10 Gy, delivered in 5 fractions over 1 week to a localized area of the tumor, ensuring enhanced tumor control.
6. Duration of Treatment: The total duration of radiotherapy was 7 weeks, with a weekend break after 5 consecutive treatment days. Patients received their radiotherapy sessions on weekdays, typically Monday through Friday, with no treatment on Saturdays and Sundays.
7. Toxicity and Side Effects: Patients were closely monitored for any radiation-induced side effects, including radiation mucositis, xerostomia (dry

[DOI: 10.61186/ijrr.23.4.4]

mouth), and skin erythema. Treatment plans were adjusted as necessary to minimize these effects, and patients received supportive care such as mouthwashes, pain management, and nutritional support.

Concomitant Treatment: In some cases, radiotherapy was combined with concurrent chemotherapy to enhance treatment effectiveness. The chemotherapy agent used was cisplatin at a dose of 40 mg/m^2 once a week during the radiotherapy course. This combination treatment is standard for locally advanced NPC to improve survival outcomes.

Statistical analysis

The raw mass data were initially preprocessed with Progenesis QI software (Waters, USA) and then analyzed using MassLynx v4.1 and MarkerLynx Application Manager (Waters Corp., Milford, MA, USA) for peak extraction, alignment, and normalization. Baseline correction was achieved by selecting the median values across all samples. Metabolites were identified and confirmed by comparing their exact mass to reference standards or by analyzing their MS/MS fragmentation patterns against data from the METLIN (http://metlin.scripps.edu), Human Metabolome Database (HMDB) (http://www.hmdb.ca/), MassBank (http://www.massbank.jp/), and LipidMaps (http://www.lipidmaps.org) databases. Data with a database similarity greater than 80% were considered appropriate.

The metaX package in R (R Core Team, Vienna, Austria) was utilized for preprocessing data, performing statistical analysis, classifying metabolites, and conducting functional annotation. Principal component analysis (PCA) was conducted to reduce the dimensionality of the multivariate dataset, enabling the identification of groups, trends (both similarities and differences within and between sample groups), and outliers. To identify differential metabolites, a multi-faceted approach was adopted: variable importance in projection (VIP) scores from the first two principal components of the partial least squares-discriminant analysis (PLS-DA) model, fold changes from univariate analysis, and Student's t-tests. Metabolites with P values less than 0.05 were considered significant, while those with P values below 0.01 were deemed highly significant. For feature selection, LASSO regression with 5-fold cross-validation was applied. Strictly speaking, biological data often deviate from a normal distribution. To enhance the reliability of the t-test results, we applied log2 transformation to the data prior to analysis, thereby approximating a normal distribution. Simultaneously, given that the differences between groups are not highly significant, the p-value was used as the criterion for screening differential metabolites to identify appropriate candidates for subsequent research, without applying multiple testing corrections [14].

RESULTS

Quality control and instrument stability

Upon overlaying the base peak ion chromatograms of all quality control (QC) samples, the chromatograms demonstrated excellent overlap in both positive and negative ion modes, with negligible variations in retention time and peak response intensity. This suggests that the instrument maintained a stable signal and remained in optimal condition throughout the entire sample detection process. Principal component analysis (PCA) of the QC samples and all other samples facilitated the assessment of the overall distribution of each sample set and the stability of the entire analytical process. As shown in figures 1A and 1B, the tighter clustering of the QC samples reflects more consistent instrument performance and enhanced data repeatability. And The corresponding RSDs, meanwhile, were all below 30%, indicating that the systematic error of this experiment was manageable.

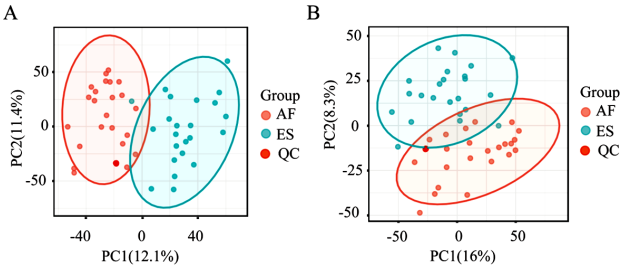

Figure 1. PCA analysis of Quality Control (QC) samples. **(A)** PCA plot for positive ion mode. **(B)** PCA plot for negative ion mode.

Compound detection results

The findings of this study revealed that, in positive ion mode, a total of 8,340 molecular features were detected in the saliva samples from both groups, with 281 features successfully identified and associated with specific compound information. In negative ion mode, a total of 5,434 molecular features were detected, of which 166 were identified and linked to corresponding compound information (table 1).

Table 1. Number of compounds and number of compounds with identification information detected in both the positive and negative ion modes.

Mode	Number of compounds	Number of compounds with identification information
Positive ionmode(pos)	8340	281
Negative ionmode(neg)	5434	166

Identification of differential metabolites

Differential metabolites between the pre- and post-radiotherapy groups were identified based on the following criteria:1) a VIP score of ≥ 1 for the first two principal components of the PLS-DA model;2) a fold-change of ≥ 1.2 or ≤ 0.83; and3) a P-value < 0.05 (figure 2).

[DOI: 10.61186/ijrr.23.4.4]

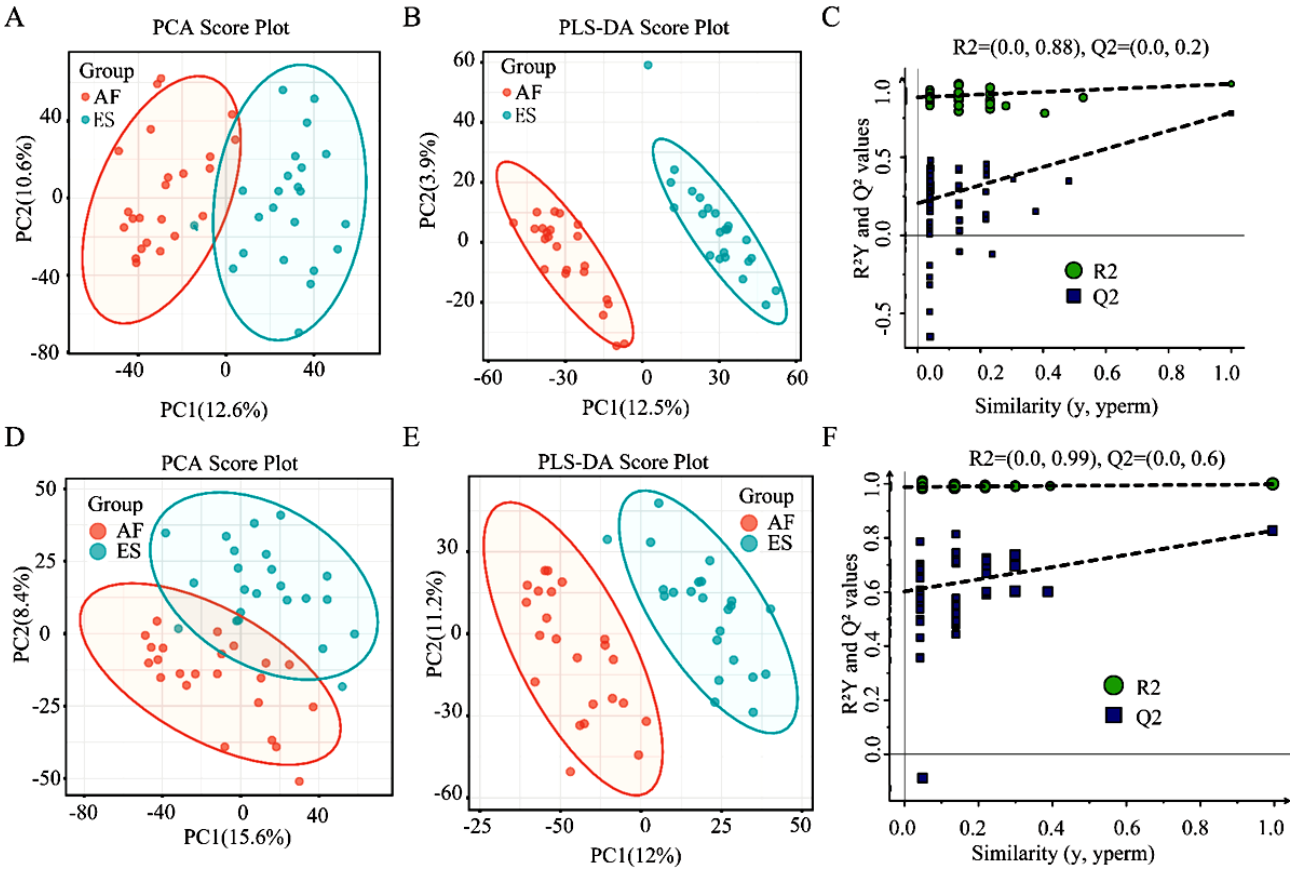

Figure 2. Multivariate analysis of salivary metabolites before and after radiotherapy. **(A, D)** PCA score plots for positive and negative ion modes, showing clustering of pre- and post-treatment samples. **(B, E)** PLS-DA score plots illustrating clear separation between groups based on metabolite profiles. **(C, F)** Validation of the PLS-DA model via permutation testing, confirming the reliability of the model (R^2Y and Q^2 values).

Through comparison between the pre- and post-radiotherapy groups, a total of 64 differential metabolites were detected in the positive ion mode, with 30 being up-regulated and 34 down-regulated. In the negative ion mode, 46 differential metabolites were identified, including 31 up-regulated and 15 down-regulated metabolites (table 2).

Table 2. Differential metabolites identified in the positive and negative ion modes

Mode	Total differential metabolites identified	Up-regulated metabolites	Down-regulated metabolites
Positive ion mode	64	30	34
Negative ion mode	46	31	15

Volcano plot and LASSO regression analysis

Perform a comprehensive analysis of the differential metabolites identified in both ion modes. As presented in table 3, among the top five up-regulated metabolites, three were associated with compounds that play biological roles and could be annotated to metabolic pathways. Among the top five down-regulated metabolites, only two were identified: one belonging to the indoles and derivatives category, and the other to keto acids and derivatives. Both of these metabolites are involved in biological processes and have been annotated to specific metabolic pathways. The above-mentioned significantly up-regulated or down-regulated metabolites with differential changes are prominently reflected in the differential volcano plot (figure 3).

Table 3. Detailed information about top5(pu1-pu5) up-regulated and top5(pd1-pd5) down-regulated differential metabolites.

	name	formula	class	KEGG
pu1	O-Acetylcarnitine	C9H18NO4		C02571
pu2	Phenyllactate	C9H10O3	Phenylpropanoic acids	C05607
pu3	9-OxoODE	C18H30O3	Fatty Acyls	C14766
pu4	Secoisolariciresinol	C20H26O6	Dibenzylbutane lignans	C18167
pu5	N,N-Dimethy-lsphingosine	C20H41NO2	Organonitrogen compounds	C13914
pd1	Lenticin	C14H18N2O2	Carboxylic acids and derivatives	C09213
pd2	Dibutyl phthalate	C16H22O4	Benzene and substituted derivatives	C14214
pd3	Indole-3-acetate	C10H9NO2	Indoles and derivatives	C00954
pd4	2-Oxoarginine	C6H11N3O3	Keto acids and derivatives	C03771
pd5	L-Phenylalanine	C9H11NO2		C00079

KEGG: Kyoto Encyclopedia of Genes and Genomes, pu1, pu2, pu3, pu4, pu5: Up-regulated metabolites, pd1, pd2, pd3, pd4, pd5: Down-regulated metabolites, C9H18NO4: Chemical formula for O-Acetylcarnitine, C9H10O3: Chemical formula for Phenyllactate, C18H30O3: Chemical formula for 9-OxoODE, C20H26O6: Chemical formula for Secoisolariciresinol, C20H41NO2: Chemical formula for N,N-Dimethylsphingosine, C14H18N2O2: Chemical formula for Lenticin, C16H22O4: Chemical formula for Dibutyl phthalate, C10H9NO2: Chemical formula for Indole-3-acetate, C6H11N3O3: Chemical formula for 2-Oxoarginine, C9H11NO2: Chemical formula for L-Phenylalanine.

[DOI: 10.61186/ijrr.23.4.4]

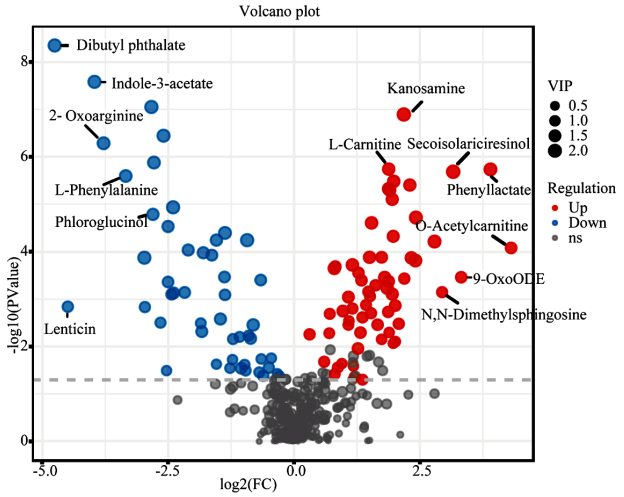

Figure 3. LASSO coefficient profile of differential salivary metabolites. Plot showing changes in metabolite coefficients with varying regularization strength (log λ). Four optimal features were selected based on λ within one standard error of the minimum mean squared error.

Subsequently, LASSO regression was employed to screen for significant metabolic differences to establish an injury profile. The data from 110 differential metabolites were analyzed using the LASSO regression with 5-fold cross-validation (figure 4). Based on the screening results and practical considerations, the lambda value corresponding to the minimum standard error (lambda. lse) was selected, yielding 4 optimal features that formed the optimal feature subset (table 4). All of four metabolites with differential changes are also prominently reflected in figure 3.

Table 4. Detailed information on the 4 optimal feature differential metabolites.

name	coefficient	formula	class	KEGG
Phloroglucinol	-0.026550681	C6H6O3	Benzene and substituted derivatives	C02183
L-Carnitine	0.008671425	C7H15NO3	Organonitrogen compounds	C00318
Kanosamine	0.182157546	C6H13NO5	Endogenous Metabolites	C12212
Dibutyl phthalate	-0.011156535	C16H22O4	Benzene and substituted derivatives	C14214

KEGG: Kyoto Encyclopedia of Genes and Genomes, coefficient: The strength of each metabolite in the model (in LASSO regression), C6H6O3: Chemical formula for Phloroglucinol, C7H15NO3: Chemical formula for L-Carnitine, C6H13NO5: Chemical formula for Kanosamine, C16H22O4: Chemical formula for Dibutyl phthalate.

Metabolic pathway enrichment analysis

The metabolic pathway enrichment analysis revealed that the top five significantly pathways in the saliva of nasopharyngeal carcinoma patients before and after radiotherapy were: arginine biosynthesis, central carbon metabolism in cancer, arginine and proline metabolism, the HIF-1 signaling pathway, and protein digestion and absorption (figure 5). As shown in table 5, arginine biosynthesis (5 metabolites hits) and arginine and proline metabolism (8 metabolites hits) fall under amino acid metabolism. The HIF-1 signaling pathway (3 metabolites hits), a hypoxia-related transcriptional signaling pathway, is closely associated with radiotherapy responses. Additionally, central carbon metabolism in cancer (6 metabolites hits) and protein digestion and absorption (5 metabolites hits) are critical in both normal physiological and pathological processes.

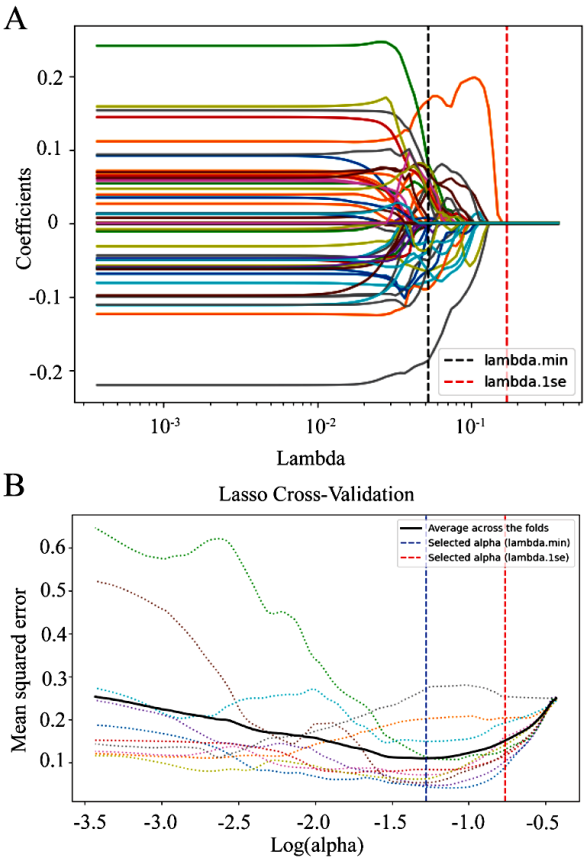

Figure 4. LASSO regression model for biomarker selection. **(A)** Coefficient trajectories of 110 differential metabolites across different λ values. **(B)** Cross-validation plot showing the mean squared error across folds, with optimal λ values (lambda.min and lambda.1se) identifying the most predictive model.

Table 5. Detailed information of the top five significantly metabolic pathways.

Name	Total metabolites	Up-regulated metabolites	Down-regulated metabolites	P value
Arginine biosynthesis	5	3	2	0.00076
Central carbon metabolism in cancer	6	3	3	0.001158
Arginine and Proline metabolism	8	6	2	0.003818
HIF-1 signaling pathway	3	2	1	0.01203
Protein digestion and absorption	5	2	3	0.018446

KEGG: Kyoto Encyclopedia of Genes and Genomes, Up-regulated metabolites: Metabolites increased in concentration after treatment, Down-regulated metabolites: Metabolites decreased in concentration after treatment.

[DOI: 10.61186/ijrr.23.4.4]

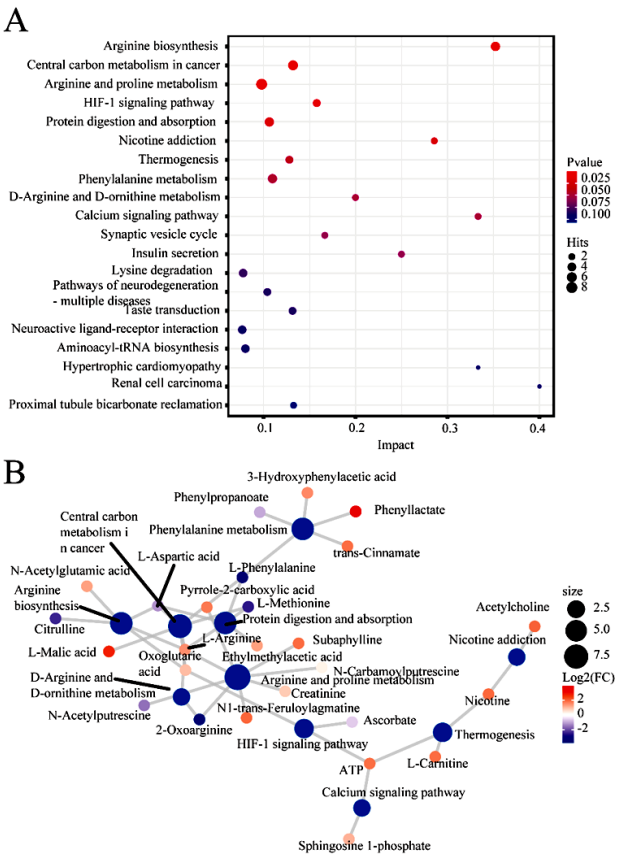

Figure 5. Metabolic pathway enrichment analysis of differential metabolites. **(A)** Enriched pathways ($p < 0.05$) in post-radiotherapy saliva samples, with enrichment factors and number of annotated metabolites per pathway. **(B)** Network map of the top five significantly enriched pathways, illustrating key metabolic responses to radiotherapy.

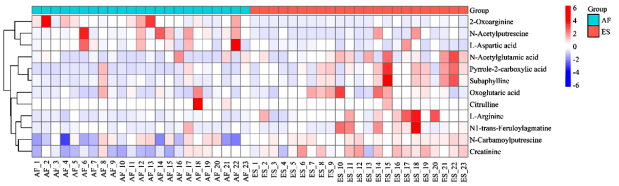

Figure 6. Heatmap of key metabolites in amino acid metabolism pathways. Heatmap showing changes in metabolite expression in arginine biosynthesis and arginine/ proline metabolism before (AF) and after (ES) radiotherapy in NPC patients.

DISCUSSION

This study provides a comprehensive metabolomic analysis of salivary alterations in nasopharyngeal carcinoma (NPC) patients undergoing radiotherapy (RT), revealing 110 significantly differential metabolites and five enriched metabolic pathways. These findings reflect the physiological and biochemical adaptations of both tumor and oral mucosal tissues during RT, offering valuable insight into the molecular underpinnings of radiation response and tissue repair. By comparing saliva samples before and after RT in the same individuals, we minimized inter-individual variability and captured dynamic, treatment-induced changes in real time.

Among the significantly altered metabolites, L-Carnitine emerged as a key upregulated compound. Known for its role in mitochondrial fatty acid transport and β-oxidation, L-Carnitine also exhibits antioxidant, anti-inflammatory, and neuroprotective effects [15]. In the context of RT, prior studies have reported that L-Carnitine supplementation helps alleviate fatigue, reduce oxidative damage, and improve treatment tolerance in cancer patients [16]. Our findings are consistent with these reports, suggesting that the observed upregulation of L-Carnitine may serve as a compensatory mechanism to support increased energy demands and repair cellular damage. Its antioxidant action also likely contributes to reducing RT-induced reactive oxygen species (ROS), preserving mitochondrial integrity, and enhancing overall cellular resilience [17, 18].

Kanosamine, another upregulated metabolite, showed a remarkable 4.5-fold increase after RT. Although relatively underexplored in human metabolism, Kanosamine has been linked to antibiotic biosynthesis pathways, including those involved in ansamycin production and microbial defense [19, 20]. Its sharp elevation suggests activation of stress-induced biosynthetic programs, potentially related to mucosal immune defense, oxidative response, or shifts in oral microbial metabolism triggered by RT. While further studies are needed to elucidate its exact role, this finding opens new avenues for understanding host-microbiota interactions during RT [21].

On the other hand, Phloroglucinol, a phenolic compound with anti-inflammatory and free radical-scavenging properties, was significantly downregulated. This likely reflects its utilization or degradation during the radiation-induced oxidative stress response [22]. Decreased levels may be due to disrupted flavonoid degradation pathways or impaired synthesis under radiotoxic conditions. Dibutyl phthalate, another downregulated metabolite, has limited biological characterization in humans and is more commonly viewed as an environmental xenobiotic. While its physiological role in RT remains unclear, its consistent reduction may indicate elimination or reduced exposure during treatment [23].

Beyond individual metabolite changes, our pathway enrichment analysis revealed significant disruptions in several fundamental metabolic pathways. Notably, arginine biosynthesis and arginine and proline metabolism were among the most significantly affected. These pathways are crucial for regulating nitric oxide production, immune responses, collagen synthesis, and redox balance [24, 25]. In our data, 12 metabolites were involved in these pathways, with a mixture of up- and

[DOI: 10.61186/ijrr.23.4.4]

downregulated trends, suggesting active metabolic reprogramming in response to radiogenic stress.

Arginine is a semi-essential amino acid vital to protein synthesis, immune cell function, and endothelial regulation through its conversion to nitric oxide [26, 27]. Increased demand for arginine during RT may reflect a need for enhanced vascular perfusion, immune surveillance, and repair. Additionally, the interconversion between arginine and proline supports cell survival and ECM remodeling during tissue recovery [28-30]. Ornithine, a shared intermediate in these pathways, plays a central role in balancing catabolic and anabolic signals during stress. The observed regulation of these metabolites is consistent with recent reports in head and neck cancer patients showing enhanced arginine turnover during RT as a compensatory response to tissue injury and hypoxia [31].

Furthermore, our analysis highlighted the HIF-1 (hypoxia-inducible factor-1) signaling pathway as significantly enriched. HIF-1 is a master transcriptional regulator activated under hypoxic conditions, and it governs genes involved in glycolysis, angiogenesis, and cell survival [32]. During RT, the rapid consumption of oxygen and subsequent tissue hypoxia lead to upregulation of HIF-1α, triggering adaptive metabolic shifts favoring anaerobic glycolysis and cell protection mechanisms [33]. Our findings align with previous studies in NPC and other cancers, where elevated HIF-1 activity correlated with poor radiotherapy response and treatment resistance [34, 35]. In addition to metabolic reprogramming, HIF-1 signaling influences immune suppression and tumor cell evasion, underscoring its role in both radioprotection and immune modulation [36, 37].

The inclusion of central carbon metabolism in cancer and protein digestion and absorption among the enriched pathways further reflects the systemic impact of RT on metabolic homeostasis. Disruption of glycolytic and amino acid pathways has been associated with treatment response and tumor progression, as cancer cells increasingly rely on metabolic plasticity to survive under therapeutic stress [36, 37]. Our data suggest that RT not only affects local oral tissues but also induces broad-spectrum shifts in host metabolism, potentially involving the tumor microenvironment, immune function, and microbial interactions.

Salivary metabolomics, as demonstrated in this study, provides a unique and non-invasive method to monitor these processes. Unlike blood or tissue biopsies, saliva offers real-time insights into local mucosal changes, systemic metabolism, and potential biomarkers for treatment response. The observed metabolic signatures—particularly changes in L-Carnitine, Kanosamine, and arginine-related pathways—may serve as valuable indicators for early detection of radiation-induced damage, mucositis progression, or treatment efficacy.

Limitations of the study

While this study offers novel insights into the metabolic consequences of radiotherapy in NPC, several limitations must be acknowledged. First, the sample size (n = 23), though suitable for preliminary analysis, limits statistical power and the generalizability of findings. Future studies with larger, multi-center cohorts are needed for validation. Second, metabolite identification relied on database annotation without targeted validation using pure standards or isotope labeling, which may introduce identification uncertainty, especially for less-characterized compounds like kanosamine. Third, while patients were instructed to follow consistent diets and oral hygiene practices, potential confounding factors such as circadian rhythm, microbiota variation, and subtle dietary influences may have affected salivary profiles. Fourth, this study focused on pre- and post-treatment comparison, but did not track intermediate or long-term changes, which may offer additional insights into recovery kinetics or late toxicity. Lastly, while we identified metabolite-pathway associations, functional validation (e.g., using transcriptomics, proteomics, or in vitro assays) was beyond the scope of this work and should be pursued in future investigations.

CONCLUSION

This study identified key salivary metabolic changes in NPC patients undergoing radiotherapy, highlighting four differential metabolites and several affected pathways related to tissue repair and stress response. These findings suggest a compensatory metabolic adaptation during treatment. Further studies with larger cohorts are needed to validate these results and explore their clinical utility.

Acknowledgments: The authors thank all patients who participated in this study and the staff of the Department of Radiation Oncology at the First Affiliated Hospital of Soochow University for their support.

Conflicts of Interest: The authors declare that they have no conflict of interest.

Funding: The National Natural Science Foundation of China (Grant No. 81703161). Jiangsu Provincial Medical Key Discipline (Grant No. ZDXK202235).

Authors contributions: L.J., collected the data and wrote the manuscript. L.W., and S.Q., collected the samples, processed and analyzed the data, and wrote the manuscript. Y.F., and J.Z., supervised the research, corrected the manuscript, and provided project funding for this work. L. J., Y.F. and J.Z., confirm the authenticity of all the raw data.

Ethical Considerations: This study was rigorously

[DOI: 10.61186/ijrr.23.4.4]

reviewed and approved by the Medical Ethics Committee of the First Affiliated Hospital of Soochow University (Approval number: (2024) Lunyan Approval No. 048).

***Possible AI usage*:** AI was employed in this study primarily to address minor grammatical and language errors, ensuring the clarity and readability of the text. Its role was limited to improving the quality of the written content without altering the scientific integrity or findings of the study.

REFERENCES

1. Sonis ST and Anderson CM (2023) Avasopasem for the treatment of radiotherapy-induced severe oral mucositis. *Expert Opin Investig Drugs, **32**(6): 463-70*.
2. Fang Y, Wang L, Chen X, Cao C (2024) Maxillary sinus anterior wall recurrence after intensity-modulated radiotherapy for nasopharyngeal carcinoma. *International Journal of Radiation Research, **22**(3): 803-5.*
3. Elad S, Yarom N, Zadik Y, Kuten-Shorrer M, Sonis ST (2022) The broadening scope of oral mucositis and oral ulcerative mucosal toxicities of anticancer therapies. *CA Cancer J Clin, **72**(1): 57-77.*
4. Wu Z, Wang B, Zhou X, Xu B, Zeng Z (2022) Radiation-induced oral mucositis is a critical dilemma for patients and physicians during radiotherapy for nasopharyngeal carcinoma. *Clinical Cancer Bulletin, **1**(2): 95-9.*
5. Tang J, Xu X, Chen M, Liu L, Zhan Z (2025) Efficacy and safety of hypofractionated radiotherapy and conventional fractionated radiotherapy in the treatment of early breast cancer patients after breast-conserving surgery. *International Journal of Radiation Research, **23**(1): 163-8.*
6. Li Y, Yang Z, Cai T, Jiang D, Luo J, Zhou Z (2023) Untargeted metabolomics of saliva in caries-active and caries-free children in the mixed dentition. *Frontiers in Cellular and Infection Microbiology, **13**: 1104295.*
7. Balakittnen J, Ekanayake Weeramange C, Wallace DF, Duijf PHG, Cristino AS, Hartel G, et al. A novel saliva-based miRNA profile to diagnose and predict oral cancer. Int J Oral Sci. 2024;16(1):14.
8. Tzimas K, Pappa E. Saliva Metabolomic Profile in Dental Medicine Research: A Narrative Review. Metabolites. 2023;13(3).
9. Liang L, Rasmussen MH, Piening B, Shen X, Chen S, Rost H, *et al*. (2020) Metabolic dynamics and prediction of gestational age and time to delivery in pregnant women. *Cell, **181**(7): 1680-92 e15.*
10. Gardner A, Carpenter G, So PW (2020) Salivary metabolomics: from diagnostic biomarker discovery to investigating biological function. *Metabolites, **10**(2): 47.*
11. Mikkonen JJ, Singh SP, Herrala M, Lappalainen R, Myllymaa S, Kullaa AM (2016) Salivary metabolomics in the diagnosis of oral cancer and periodontal diseases. *J Periodontal Res, **51**(4): 431-7.*
12. Buzalaf MAR, Ortiz AdC, Carvalho TS, Fideles SOM, Araújo TT, Moraes SM, *et al.* (2020) Saliva as a diagnostic tool for dental caries, periodontal disease and cancer: is there a need for more biomarkers? *Expert Review of Molecular Diagnostics, **20**(5): 543-55.*
13. Kim S, Kim HJ, Song Y, Lee HA, Kim S, Chung JJJocp (2021) Metabolic phenotyping of saliva to identify possible biomarkers of periodontitis using proton nuclear magnetic resonance. *Journal of Clinical Periodontology, **48**(9): 1240-9.*
14. Zheng WB, Zou Y, Elsheikha HM, Liu GH, Hu MH, Wang SL, *et al.* (2019) Serum metabolomic alterations in Beagle dogs experimentally infected with Toxocara canis. *Parasit Vectors, **12**(1): 447*.
15. Fritz IB, Yue KT. Long-Chain Carnitine Acyltransferase and the Role of Acylcarnitine Derivatives in the Catalytic Increase of Fatty Acid Oxidation Induced by Carnitine. J Lipid Res. 1963;4:279-88.
16. Graziano F, Bisonni R, Catalano V, Silva R, Rovidati S, Mencarini E, *et al.* (2002) Potential role of levocarnitine supplementation for the treatment of chemotherapy-induced fatigue in non-anaemic cancer patients. *Br J Cancer, **86**(12): 1854-7*.
17. Kraft M, Kraft K, Gärtner S, Mayerle J, Simon P, Weber E, *et al*. (2012) L-Carnitine-supplementation in advanced pancreatic cancer (CARPAN)--a randomized multicentre trial. *Nutrition Journal, **11**: 52*.
18. Longo N, Frigeni M, Pasquali M (2016) Carnitine transport and fatty acid oxidation. *Biochim Biophys Acta, **1863**(10): 2422-35*.
19. Mahmud T (2003) The C7N aminocyclitol family of natural products. *Nat Prod Rep, **20**(1): 137-66.*
20. Kudo F and Eguchi T (2009) Biosynthetic genes for aminoglycoside antibiotics. *J Antibiot (Tokyo), **62**(9): 471-81.*
21. Vijayalaxmi S, Jayalakshmi SK, Sreeramulu K (2015) Polyphenols from different agricultural residues: extraction, identification and their antioxidant properties. *Journal of Food Science and Technology, **52**(5): 2761-9.*
22. Benjamin S, Masai E, Kamimura N, Takahashi K, Anderson RC, Faisal PA (2017) Phthalates impact human health: Epidemiological evidences and plausible mechanism of action. *J Hazard Mater, **340**: 360-83.*
23. Wu G, Bazer FW, Davis TA, Kim SW, Li P, Marc Rhoads J, *et al.* (2009) Arginine metabolism and nutrition in growth, health and disease. *Amino Acids, **37**(1): 153-68*.
24. Morris SM, Jr. (2016) Arginine metabolism revisited. *J Nutr, **146**(12): 2579S-86S*.
25. Geiger R, Rieckmann JC, Wolf T, Basso C, Feng Y, Fuhrer T, *et al*. (2016) L-arginine modulates T cell metabolism and enhances survival and anti-tumor activity. *Cell, **167**(3): 829 -42 e13*.
26. Song CW, Shakil A, Osborn JL, Iwata K (2009) Tumour oxygenation is increased by hyperthermia at mild temperatures. *International Journal of Hyperthermia, **25** (2): 91-5.*
27. Xiong L, Teng JL, Botelho MG, Lo RC, Lau SK, Woo PC (2016) Arginine metabolism in bacterial pathogenesis and cancer therapy. *Int J Mol Sci, **17**(3): 363*.
28. Wu G, Bazer FW, Burghardt RC, Johnson GA, Kim SW, Knabe DA, *et al.* (2011) Proline and hydroxyproline metabolism: implications for animal and human nutrition. *Amino Acids, **40**(4): 1053-63.*
29. Phang JM, Donald SP, Pandhare J, Liu Y (2008) The metabolism of proline, a stress substrate, modulates carcinogenic pathways. *Amino Acids, **35**(4): 681-90.*
30. Phang JM, Liu W, Hancock CN, Fischer JW (2015) Proline metabolism and cancer: emerging links to glutamine and collagen. *Curr Opin Clin Nutr Metab Care, **18**(1): 71-7.*
31. Horsman MR and Overgaard J (2016) The impact of hypoxia and its modification of the outcome of radiotherapy. *J Radiat Res, **57**; Suppl 1(Suppl 1): i90-i8.*
32. Semenza GL (2012) Hypoxia-inducible factors in physiology and medicine. *Cell, **148**(3): 399-408.*
33. Balamurugan K (2016) HIF-1 at the crossroads of hypoxia, inflammation, and cancer. *International Journal of Cancer, **138**(5): 1058-66.*
34. Gray LH, Conger AD, Ebert M, Hornsey S, Scott OJTBjor (1953) The concentration of oxygen dissolved in tissues at the time of irradiation as a factor in radiotherapy. *Br J Radiol, **26**(312): 638-48.*

[DOI: 10.61186/ijrr.23.4.4]

35. Kim JW, Tchernyshyov I, Semenza GL, Dang CV (2006) HIF-1-mediated expression of pyruvate dehydrogenase kinase: a metabolic switch required for cellular adaptation to hypoxia. *Cell Metab,* ***3****(3): 177-85*.
36. Noman MZ, Desantis G, Janji B, Hasmim M, Karray S, Dessen P, *et al*. (2014) PD-L1 is a novel direct target of HIF-1α, and its blockade under hypoxia enhanced MDSC-mediated T cell activation. *The Journal of Experimental Medicine,* ***211****(5): 781-90*.
37. Labiano S, Palazón A, Bolaños E, Azpilikueta A, Sánchez-Paulete AR, Morales-Kastresana A, *et al*. (2016) Hypoxia-induced soluble CD137 in malignant cells blocks CD137L-costimulation as an immune escape mechanism. *Oncoimmunology,* ***5****(1): e1062967*.

[DOI: 10.61186/ijrr.23.4.4]